

Sulfonated Poly(ether sulfone)-Based Catalyst Binder for a Proton-Exchange Membrane Fuel Cell

N. Nambi Krishnan, Hyoung-Juhn Kim, Jong Hyun Jang, Sang-Yeop Lee, EunAe Cho, In-Hwan Oh, Seong-Ahn Hong, Tae-Hoon Lim

Center for Fuel Cell Research, Korea Institute of Science and Technology, 39-1 Hawolgok-Dong, Sungbuk-Gu, Seoul 136-791, South Korea

Received 16 September 2008; accepted 26 January 2009

DOI 10.1002/app.30296

Published online 28 April 2009 in Wiley InterScience (www.interscience.wiley.com).

ABSTRACT: Sulfonated poly(ether sulfone) copolymer (PES 60) and its partially fluorinated analogue (F-PES 60) were synthesized via the nucleophilic aromatic polycondensation of commercially available monomers to make a polymer electrolyte membrane and a binding material in the electrodes of a membrane–electrode assembly (MEA). PES 60 and F-PES 60 showed proton conductivities of 0.091 and 0.094 S/cm, respectively, in water at room temperature. The copolymer was dissolved in the mixture of alcohol and water to get a 1 wt % binder solution. A catalyst slurry was prepared with the copolymer solution and sprayed on the copol-

ymers (PES 60 or F-PES 60) membrane to obtain a MEA. Both PES 60 and F-PES 60 based MEAs were fabricated with different amounts of their binder in the electrodes to examine the effect of the copolymer binder in the catalyst layer on the fuel cell performance. The MEA with 2 wt % copolymer binder in the electrodes showed the best fuel cell performance. © 2009 Wiley Periodicals, Inc. *J Appl Polym Sci* 113: 2499–2506, 2009

Key words: electrochemistry; membranes; co-polymer binder; poly(ether sulfone)s; proton exchange membrane fuel cell

INTRODUCTION

Proton-exchange membrane fuel cells (PEMFCs) have been widely investigated as automotive, stationary, and portable power sources because of their high conversion efficiency and environmental friendliness. Among several components of a PEMFC, the polymer electrolyte membrane is one of the most important parts. In the past few decades, DuPont's Nafion membrane has been used mostly as a polymer electrolyte for PEMFCs because of its high ionic conductivity, high mechanical strength, and chemical stability. However, it still has some problems. Its proton conductivity is low at high temperatures under low humidity. Also, it is very expensive. For these reasons, hydrocarbon-based, proton-conducting polymers have been investigated as alternatives. Although a huge number of polymeric syntheses and their sufficient characterizations with fuel cell results have been reported, additional advancements are required to meet the demands of fuel cells in both stationary and automotive operations. Alternative high-performance polymers (hydrocarbon-based polymers), such as sulfonated poly(aryl ether sulfone)s, poly(aryl ether ketone)s, poly(ether imide)s, polybenzimidazole, poly(phenylene oxide), and poly(phenylene sulfide) are well known for their excel-

lent thermal, mechanical, and oxidative stabilities.^{1–3} Rikukawa and Sanui² and Hickner et al.³ extensively reviewed high-performance polymers for polymer electrolyte membranes.

Nafion ionomers are used as a catalyst binding material in electrodes because Nafion chemical inertness improves stability and its high proton-conductivity properties improve access to the Pt catalyst in PEMFC electrodes. Also, hydrocarbon-based polymer membranes have been demonstrated for fuel cell operations with a Nafion binder in the catalyst layers.^{4–14} However, the systems containing Nafion binder exhibited poor interfacial compatibility between the membrane and electrodes.⁴ Therefore, the use of hydrocarbon-based polymers as binders in the catalyst layer is emerging as a new area of research. Recently, sulfonated poly(ether ether ketone) (PEEK), poly(arylene ether sulfone) (PAES), and polybenzimidazole (PBI) have been reported as binder materials in the catalyst layer. Easton et al.¹⁵ studied the effect of sulfonated PEEK ionomer in the electrocatalytic layer. The interfacial resistance was reduced when the ionomer was incorporated into the catalyst layer. Jung and coworkers^{16,17} demonstrated the long-term stability of sulfonated PEEK and PAES membranes with binders that were made with their corresponding polymers. Seland et al.¹⁸ showed that a membrane–electrode assembly (MEA) with the anode layer containing 0.4 mg of Pt/cm² with 0.36 mg of PBI/cm² and the cathode layer containing 0.6 mg of Pt/cm² with 0.6 mg of PBI/cm²

Correspondence to: H.-J. Kim (hjkim25@kist.re.kr).

had the best single-cell performance under certain operating conditions.

In our previous work, we reported the PEMFC, direct methanol fuel cell, and direct formic acid fuel cell performances of MEAs with a sulfonated poly(ether sulfone) copolymer (PES 60) membrane with a Nafion binder in the catalyst layers.^{12,13} In this article, we describe the cell performance of a MEA with PES 60 and its partially fluorinated analogue (F-PES 60) with corresponding copolymer binders. Sasikumar et al.¹⁹ found that the single-cell performance depended on the ratio of the binding ionomer to catalyst loading amount. A significant improvement in the single-cell performance was achieved with the use of Nafion membranes with optimum Nafion ionomer contents in the catalyst layer. We changed the ratio between the hydrocarbon-based polymer binder and Pt catalyst to determine the optimum content for the binding polymer in the catalyst layers.

EXPERIMENTAL

Materials

Hydroquinone 2-potassium sulfonate (HPS), bis(4-fluorophenyl)sulfone (FPS), bisphenol A (BPA), and anhydrous potassium carbonate were obtained from Aldrich (St. Louis, MO). 2,2-Bis(4-hydroxyphenyl)hexafluoropropane (6F-BPA) was purchased from TCI (Tokyo, Japan). The HPS was recrystallized from deionized water before use. Potassium carbonate, FPS, BPA, HPS, and 6F-BPA were dried at 60°C for 24 h *in vacuo* before polymerization. Dimethylacetamide (DMAc), dimethyl sulfoxide (DMSO), *N*-methyl-2-pyrrolidone (NMP; Sigma-Aldrich), toluene, HCl (J. T. Baker, USA), 1-propanol, 2-propanol (Aldrich, high performance liquid chromatography (HPLC) grade), and methanol (Daejung Reagents & Chemicals, Siheung City, Korea) were used as received.

Synthesis of BPA- and 6F-BPA-based PES 60 and F-PES 60

The salt-form PES 60 and F-PES 60 were synthesized with a method that was described elsewhere.¹² The copolymerization procedure for F-PES 60 is explained as follows: first, FPS (5.09 g, 20 mmol), 6F-BPA (2.69 g, 8 mmol), HPS (2.74 g, 12 mmol), and potassium carbonate (5.7 g, 40 mmol) were added to a mixture of 25 mL of DMAc and 40 mL of toluene in a 100-mL, round-bottom flask equipped with a magnetic stirrer, Dean-Stark trap, condenser, nitrogen inlet, and thermometer. The reaction mixture was refluxed at 150°C for 4 h to dehydrate the system. The temperature was raised slowly to 180–185°C by the controlled removal of the toluene. After the complete removal of the toluene, the reaction was allowed to proceed until a vis-

cous solution was formed. The viscous solution was cooled to room temperature and poured into 1000 mL of methanol to obtain the F-PES copolymer. The copolymer was then collected by vacuum filtration and dried in a vacuum oven at 60°C for 1 h. Then, the copolymer was subjected to Soxhlet extraction with deionized water to remove inorganic material. Finally, the salt-form copolymer was dried in the vacuum oven at 60°C for 24 h.

¹H-NMR (PES 60, δ , DMSO-*d*₆): 1.65 (s, 6H, —CH₃), 6.96–7.35 (m, 21H, ArH), 7.37–7.52 (m, 1.5H, ArH), 7.80–8.02 (m, 10H, ArH). ¹H-NMR (F-PES 60, δ , DMSO-*d*₆): 6.98–7.32 (m, 17H, ArH), 7.37–7.53 (m, 5.5H, ArH), 7.79–8.10 (m, 10H, ArH). Fourier transform infrared (FTIR) spectroscopy (PES 60 cm⁻¹): 712, 1020, 1078, 1107, 1146, 1225, 1476, 1584. FTIR (F-PES 60 cm⁻¹): 832, 1019, 1076, 1104, 1145, 1229, 1470, 1584.

Membrane preparation and acidification of the sulfonated poly(ether sulfone)s

The salt form of PES 60 (or F-PES 60) was dissolved in DMSO at room temperature (15% w/v). Then, the solution was filtered and poured onto a clean glass plate. The thickness of the solution on the glass plate was controlled by a doctor blade. The membrane was dried at 60°C under reduced pressure (76 cmHg) for 30 h. The membrane was removed from the glass plate by immersion in deionized water. It was acidified with 10% HCl solution at 60°C for 2 h and rinsed with deionized water several times. Finally, the membrane was stored in deionized water at room temperature.

Ion-exchange capacity (IEC), water uptake, and solubility in boiling water

The IEC of the membranes (PES 60 and F-PES 60) was determined by a titration method. A dried membrane of 1 g was soaked in 1M NaCl solution for 24 h to exchange the proton of the sulfonic acid group with a sodium ion. The exchanged proton was titrated with a 0.01M NaOH solution with phenolphthalein as an indicator. The moles of the proton were equal to the moles of the sulfonic group. From the titration value, IEC was calculated from the following equation:

$$\text{IEC} = \frac{C_{\text{NaOH}} V_{\text{NaOH}}}{W_m} \quad (1)$$

where C_{NaOH} , V_{NaOH} , and W_m are the concentration of NaOH solution, the consumed volume of NaOH solution, and the weight of the membrane, respectively. IEC is expressed as milliequivalents of sulfonic acid per gram of dry polymer.

The water uptake was determined for the PES 60 and F-PES 60 membranes. The membranes were first

dried at 120°C for 24 h under reduced pressure. They were immersed in water at 30°C for 48 h. The water uptake was calculated from the following equation:

$$\text{Water uptake} = \frac{W_{\text{wet}} - W_{\text{dry}}}{W_{\text{dry}}} \times 100 \quad (2)$$

where W_{wet} and W_{dry} are the weights of the wet and dry membranes, respectively.

The solubility in boiling water of the membranes (PES 60 and F-PES 60) was tested with a Soxhlet extractor. The membrane was dried at 120°C for 24 h under reduced pressure. The weight and size of the membrane were measured. Then, the membrane was placed in a Soxhlet extractor with deionized water for 48 h. Finally, the membrane was removed from the extractor and dried under the same conditions. The change in the membrane was measured.

Proton conductivity

A Zahner Elektrik IM6 (ZAHNER-elektrik GmbH, Kronach, Germany) impedance spectrometer was used in galvanostatic mode with an alternating-current amplitude of 1 mA (current = 0 A) over a frequency range of 1 Hz–5 MHz. The acid-form membrane resistance was measured under fully hydrated conditions with a four-point-probe conductivity cell.²⁰ The proton conductivity (σ) was calculated via the following equation:

$$\sigma(\text{S/cm}) = \frac{L(\text{cm})}{R(\Omega) \times A(\text{cm}^2)} \quad (3)$$

where L is the distance between the two potential probes, R is the ion-conductive resistance of the membrane from the impedance spectra, and A is the membrane cross-sectional area (Thickness \times Width).

Techniques

The functional groups of PES 60 and F-PES 60 were confirmed from the FTIR spectroscopic technique. The FTIR measurement was recorded with a Thermo Mattson Infinity Gold FTIR 60 AR model spectrometer (Varian Associates, Palo Alto, CA). The ¹H-NMR (300-MHz) (Thermo Scientific Inc., USA) spectrum was recorded on a Varian instrument at room temperature in DMSO-*d*₆ with tetramethylsilane as an internal standard. The thermal stability was analyzed by means of thermogravimetric analysis (TGA) with a TGA 2050 V5.2B instrument (Instruments Specialists, Inc., USA) (heating rate = 10°C/min). Proton-conductivity measurements were performed on the acid forms of the membranes. The proton conductivities of these membranes were measured with the method of Sumner et al.²⁰

Preparation of the binder solution

A binder solution of 1 wt % was prepared in a Teflon container, which was placed inside a stainless steel vessel. The acid form of the copolymer (0.5 g of PES 60 or F-PES 60) was placed in a mixture of 30 g of deionized water and 10 g of 1-propanol and 2-propanol in the container. The stainless vessel was closed tightly and placed in an oil bath. The solution was stirred, and the oil bath temperature was maintained at 70°C for 12 h. The solution was cooled to room temperature. Finally, the homogeneous clear solution was carefully transferred into a glass bottle, and the solution was stored at room temperature.

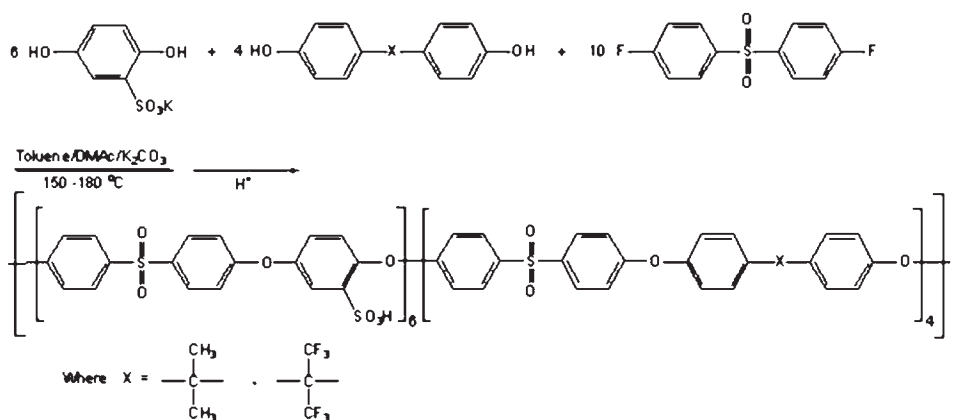
Preparation of the MEA and the single-cell test

The catalyst slurry was prepared by the mixture of 40 wt % Pt on Vulcan XC-72 (E-Tek, Inc., USA) catalyst power with 2-propanol. The mixture was ultrasonicated for 1 h. The 1 wt % copolymer binder solution (PES 60 or F-PES 60) was added to the catalyst slurry; this was sonicated again for 1 h. To examine the effect of binder content to the catalyst in the electrodes, the binder content to the catalyst was varied from 1.5 to 32 wt %. We prepared the catalyst-coated membrane (CCM) by spray-coating the prepared catalyst slurry on the acid form of the membrane. The Pt loadings were fixed at 0.2 mg/cm² for the anode and 0.4 mg/cm² for the cathode with different amounts of binder in the catalyst layer. Finally, the CCM was dried at 60°C for 5 h.

The single cell was fabricated with the CCM, the gas diffusion media Sigracet SGL 10BC (Meitigen, Germany), Teflon gaskets, and graphite blocks. The gases (fuel and oxidant with flow rate of 400 mL/min under ambient pressure) were passed through bubble humidifiers at temperatures of 70°C (anode) and 65°C (cathode) before entry via the fuel cell inlets. The active electrode area for the single-cell test was 25 cm². The cell temperature was 70°C. Current–potential characteristics were evaluated with an electric load (Daegil Electronics, EL500P, Seoul, Korea).

Cell impedance measurement

Electrochemical impedance spectra were recorded with an IM6 Zahner Elektrik instrument. The single cell was operated at 70°C, and the applied frequency was varied from 10 kHz to 10 mHz with an alternating-current amplitude of 5 mV. Humidified oxygen and hydrogen gases with a flow rate of 400 mL/min were applied to cathode and anode, respectively, at ambient pressure.



Scheme 1 Synthesis of PES 60 and F-PES 60.

RESULTS AND DISCUSSION

Synthesis and characterization of the poly(ether sulfone)s (PES 60 and F-PES 60)

Two types of sulfonated poly(ether sulfone) were prepared by the modified method described in the ref. 21. The degree of sulfonation of a polymer electrolyte influences the conductivity of the electrolyte membrane and its solubility in water. In this study, we used 60 mol % hydrophilic parts containing copolymers for the high proton conductivity and water insolubility in boiling water. The PES 60 and F-PES 60 polymers were prepared by the direct synthesis of FPS with stoichiometric amounts of hydroxyl-group-terminated monomers (HPS and BPA or 6F-BPA) in the presence of potassium carbonate in DMAc (Scheme 1).

The chemical structure of F-PES 60 was confirmed by FTIR and $^1\text{H-NMR}$ analyses. The FTIR spectrum of F-PES 60 is presented in Figure 1. The characteristic absorption band for the aromatic sulfone group appeared at 1145 cm^{-1} , and the peak for aryl oxide appeared at 1229 cm^{-1} .²² The peaks at 1584 and 1470 cm^{-1} were attributed to the vibration of the aromatic ring skeleton.²³ The two absorption peaks appearing at 1076 and 1019 cm^{-1} were characteristic of the aromatic SO_3^- stretching vibrations.²⁴

Four different kinds of aromatic hydrogens of F-PES 60 were observed at $6.98\text{--}8.10\text{ ppm}$ in $^1\text{H-NMR}$ (Fig. 2). The range of chemical shift clearly exhibited the separation of the aromatic hydrogens, which were ortho in position to the ether linkages ($<7.32\text{ ppm}$), and the aromatic hydrogens, which were ortho in position to the sulfone groups (over 7.79 ppm). For PES 60, aromatic hydrogen, which was ortho in position to the sulfonic acid group, appeared at $7.37\text{--}7.53\text{ ppm}$.¹² However, the aromatic hydrogen, noted as "a" in the repeating unit of F-PES 60 in Figure 2, was not well separated in the region. Presumably, the signal corresponding to the hydrogen "a" and the signal corresponding to the

hydrogen "b" in the repeating unit overlapped. Theoretically, the peak integration values for aromatic hydrogens of "a" and "b", ortho in position to the ether linkages and ortho in position to the sulfone linkages, were 1.5H , 4H , 17H , and 10H , respectively. The integration value obtained by $^1\text{H-NMR}$ showed the same value.

TGA was performed on F-PES 60 (acid form) to evaluate its thermal stability (Fig. 3). The TGA curve indicated that the weight loss up to 200°C appeared to be due to water evaporation, whereas the weight loss at about 300°C was attributed to the degradation of the sulfonic group. The third weight loss occurred around 510°C , which was due to the decomposition of the polymer backbone. Compared to PES 60, the temperature for desulfonation increased by about 30°C .¹² Harrison et al.²⁵ reported that the first weight loss due to desulfonation processes was observed beyond 350°C for disulfonated PAES copolymers. The TGA result indicated that the

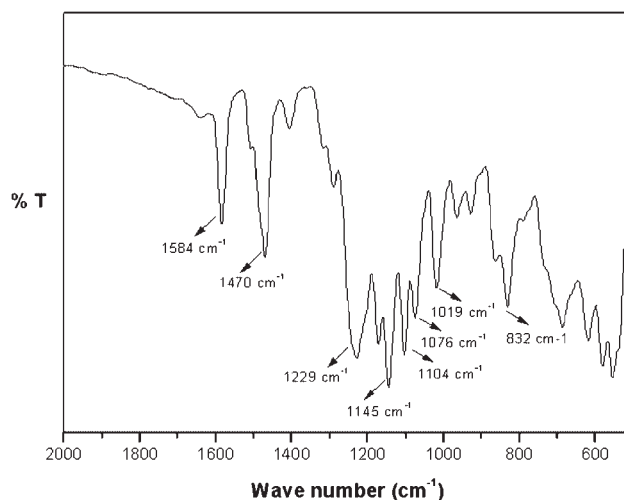


Figure 1 FTIR spectrum of the acid-form F-PES 60 membrane.

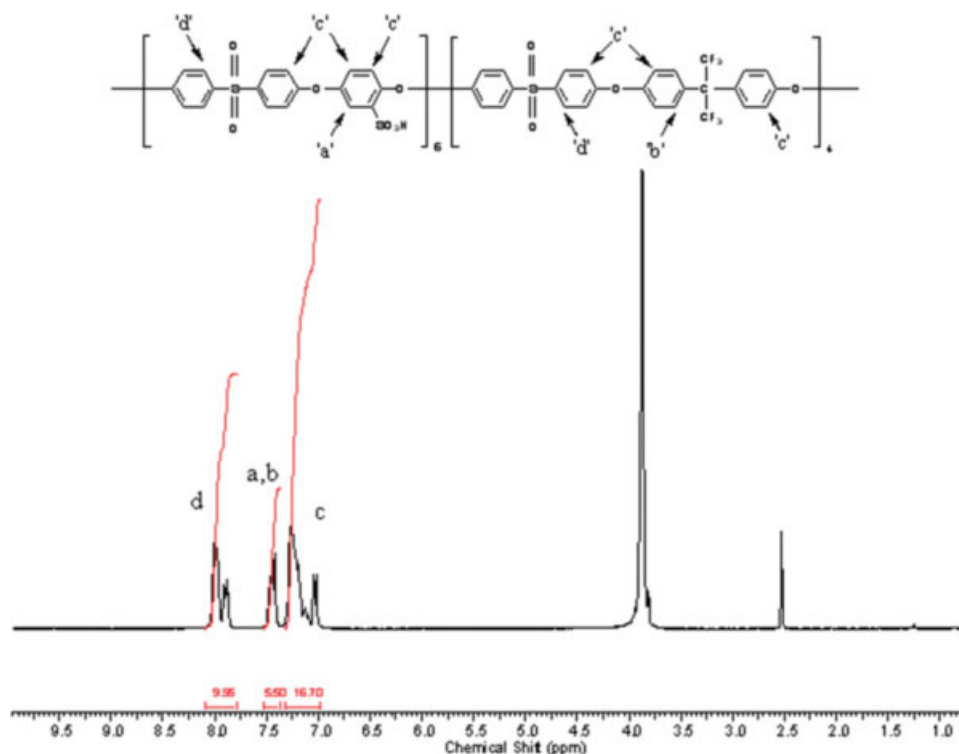


Figure 2 $^1\text{H-NMR}$ spectrum of the acid-form F-PES 60 membrane. [Color figure can be viewed in the online issue, which is available at www.interscience.wiley.com.]

sulfonated F-PES 60 was thermally stable for the temperature range of PEMFC application.

Single-cell performance of the sulfonated poly(ether sulfone) binder based MEAs

To operate a PEMFC, the proton-exchange membrane should have properties such as a high proton conductivity and chemical and thermal stability. Interestingly, PES 60 and F-PES 60 had high proton conductivities of over 10^{-2} S/cm. The incorporation of fluorine increased the proton conductivity and lowered water uptake. The basic properties of the membrane, including IEC, water uptake, proton conductivity, and solubility in solvents of the copolymers, are listed in Table I. The weights and sizes of the membranes (PES 60 and F-PES 60) were unchanged after Soxhlet extraction. This indicated good water insolubility in the membranes.

The polarization curves of the MEA with various PES 60 binder loadings on the PES 60 membrane are shown in Figure 4. As shown in this figure, the fuel cell performance increased with decreasing PES 60 binder loading up to 2 wt %. The polarization curves for the F-PES 60 based MEA are shown in Figure 5, in which the 2 wt % binder containing F-PES 60 MEA also showed the best cell performance. As the F-PES 60 binder increased in the electrode, a similar decreasing trend was observed in the fuel cell per-

formance. The polarization curve of a typical fuel cell consists of three zones based on the overpotential. The dominant losses in low over potential or low current density region are due to electrode kinetics. In the middle range, the ohmic contributions play an important role, and at the high-current-density regions, mass transport limitations become dominant. A comparison of the single-cell performance of the PES 60 binder based MEAs and F-PES 60 binder based MEAs indicated that they

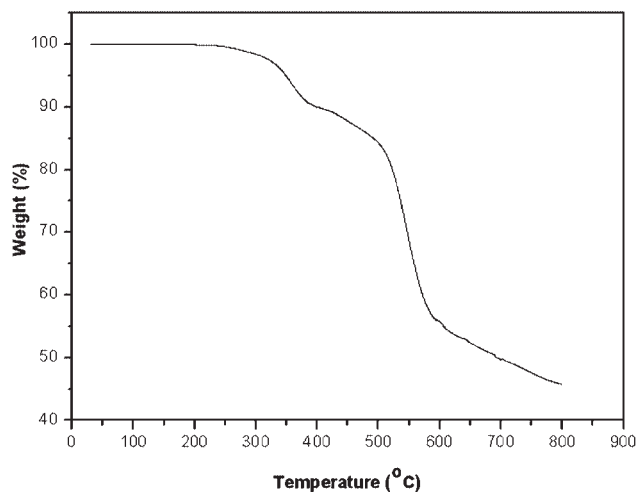


Figure 3 TGA curve of the acid-form F-PES 60 membrane.

TABLE I
Basic Membrane Properties of the Sulfonated Poly(ether sulfone) Copolymers

Acid-form polymer membrane	Solubility ^a	Solubility ^b	IEC (mequiv/g)	Water uptake (wt %)	Proton conductivity (S/cm) ^c
PES 60	X	O	1.43	30	0.091
F-PES 60	X	O	1.28	23	0.094

X = not soluble; O = soluble.

^a Solubility in boiling water (Soxhlet extraction).

^b Solubility in aprotic solvents (DMAc, DMSO, and NMP) at room temperature.

^c Proton conductivity at room temperature.

had similar polarization behaviors. Electrodes based on alternative binders may have significantly poor electrode kinetics.

The requirement for an electrolyte used as a membrane is different from that for an electrolyte used in the catalyst layer. In the catalyst layer, the transport of reactants, protons, and electrons, that is, the formation of a triple-phase boundary, is essential for obtaining high Pt utilization. Therefore, the electrolyte used in the catalyst layer must be reactant-permeable, whereas the electrolyte used in the membrane requires no reactant permeability.²⁶ Presumably, the 2 wt % binder containing MEAs had better triple-phase boundary formation than the others. This may have been the reason for their better fuel cell performance. The fuel cell performance of the PES 60 binder based MEA was very low compared to that of the Nafion-binder-based MEA.^{12,13} The Nafion binder had the hydrophobic polytetrafluoroethylene-like backbone, which aided in pore formation and water management.¹⁵ The oxygen reduction reaction kinetics in the Nafion system were higher than in other sulfonated polymers.²⁷ Zhang et al.²⁸

reported the oxygen reduction kinetics and transport properties at the Pt/membrane interface with both Nafion 117 (IEC = 0.91 mequiv/g) and sulfonated PAES (SPES-40, IEC = 1.72 mequiv/g) membranes. They found that the oxygen permeability of Nafion 117 was 1.5–3 times higher than that of PES-40. Easton et al.¹⁵ found that the oxygen permeability of Nafion was five times higher than that of sulfonated PEEK. Therefore, the Nafion-binder-based MEA showed a much higher performance than the alternative-binder-based MEA.

Impedance of the H₂/O₂ cells under polarization

The impedance spectra obtained for the MEAs with various amount of sulfonated poly(ether sulfone) on the corresponding membrane (PES 60 and F-PES 60) are shown in Figures 6 and 7. The ohmic resistance and charge-transfer resistance values of the MEAs are shown in Table II. The impedance spectra exhibited distinct arcs. The intercept of the high-frequency arc with the real axis represents the total ohmic

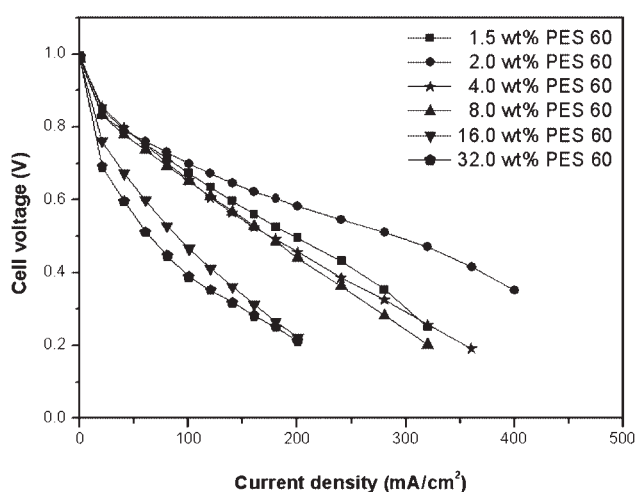


Figure 4 H₂/O₂ single-cell performance of MEAs with PES 60 membranes and binders in catalyst layers: catalyst loadings = 0.2 mg/cm² (anode) and 0.4 mg/cm² (cathode); cell temperature = 70°C; humidified fuel and oxidant fed with a flow rate of 400 mL/min under ambient pressure.

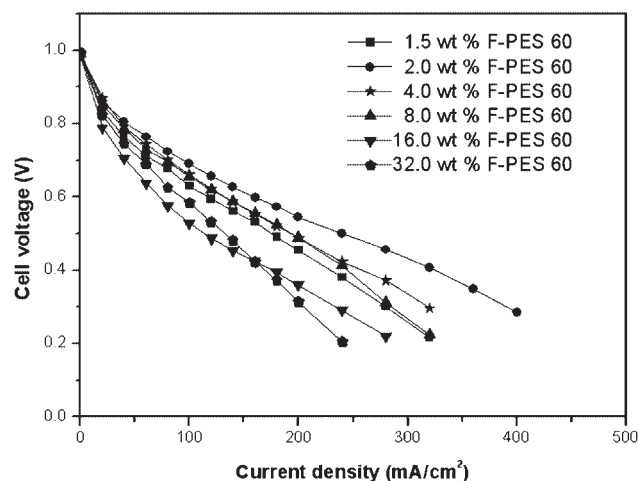


Figure 5 H₂/O₂ single-cell performance MEAs with F-PES 60 membranes and binders in catalyst layers: catalyst loadings = 0.2 mg of Pt/cm² (anode) and 0.4 mg of Pt/cm² (cathode); cell temperature = 70°C; humidified fuel and oxidant fed with a flow rate of 400 mL/min under ambient pressure.

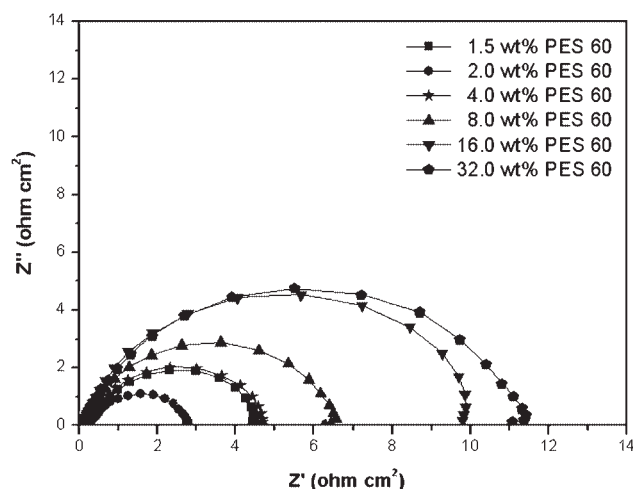


Figure 6 Impedance analyses at 0.85 V of cells with various PES 60 binder loadings for H₂/O₂ cells. Z' and Z'' are the real and imaginary parts of impedance, respectively.

resistance of the cell. The ohmic resistance of the cell is expressed as the sum of the contributions from the uncompensated contact resistance and the ohmic resistance of the cell components, that is, the membrane, catalyst layer, and so on. The diameter of the low-frequency arc represents the charge-transfer resistance across the electrode–electrolyte interface and is inversely proportional to the rate of the oxygen reduction reaction.^{29,30} At a fixed cell voltage of 0.85 V, the total ohmic resistance values for the PES 60 binder based MEAs varied from 0.08 to 0.15 $\Omega \text{ cm}^2$. The total ohmic resistance values for the F-PES 60 binder based MEAs varied from 0.13 to 0.17 $\Omega \text{ cm}^2$. This might have been due to the internally distributed ohmic resistance and the contact capacitance. In

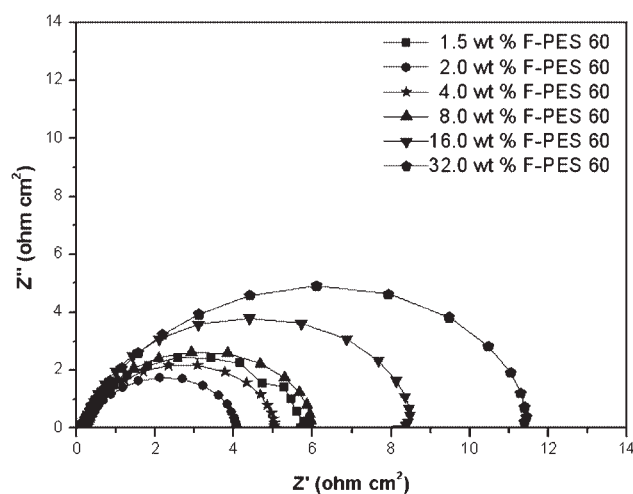


Figure 7 Impedance analyses at 0.85 V of cells with various F-PES 60 binder loadings for H₂/O₂ cells. Z' and Z'' are the real and imaginary parts of impedance, respectively.

TABLE II
Electrochemical Properties of the Different Amounts of Binder to the Catalyst of the MEAs

	Amount of binder to the catalyst	Ohmic resistance ($\Omega \text{ cm}^2$)	Charge-transfer resistance ($\Omega \text{ cm}^2$)
PES 60	1.5	0.15	4.3
	2.0	0.08	2.7
	4.0	0.14	4.5
	8.0	0.14	6.3
	16.0	0.11	9.7
	32.0	0.10	11.2
F-PES 60	1.5	0.14	5.6
	2.0	0.15	3.9
	4.0	0.16	4.9
	8.0	0.17	5.7
	16.0	0.14	8.2
	32.0	0.13	11.3

both cases, the impedance analysis revealed that the charge-transfer resistance was the lowest when 2.0 wt % binder (2.7 $\Omega \text{ cm}^2$ for PES 60 and 3.9 $\Omega \text{ cm}^2$ for F-PES 60) was loaded in the electrodes. The diameter of the semicircle increased rapidly with increasing ionomer (PES 60 and F-PES 60) loadings in the electrodes. It was clear that electrodes based on the alternative ionomer had poor interfacial kinetics. Probably, the catalyst utilization decreased with higher ionomer loadings, so the oxygen reduction polarization increased. This could have been the reason behind the low fuel cell performance.

CONCLUSIONS

Partially fluorinated and nonfluorinated poly(ether sulfone) copolymers with 60 mol % hydrophilic parts in their repeating unit were synthesized successfully. The proton conductivity, thermal stability, and water insolubility of the copolymers indicated their possibility for PEMFC operation. In this study, the role of the copolymers as electrolytes and binding materials was examined. The polarization curve and impedance spectra provided an understanding of the influence of this alternative binder material loading on the fuel cell performance. In both cases, 2 wt % ionomer in the catalyst layer showed the best fuel cell performance. However, the incorporation of the PES 60 or F-PES 60 binder in the catalyst layer led to low fuel cell performance compared to that of the Nafion binder system. This article promotes the next objective of our work, to investigate the polymer structure, which can act as both an electrolyte and a binder for fuel cell applications.

References

1. Kerres, J. A. *J Membr Sci* 2001, 185, 3.

2. Rikukawa, M.; Sanui, K. *Prog Polym Sci* 2000, 25, 1463.
3. Hickner, M. A.; Ghassemi, H.; Kim, Y. S.; Einsla, B. R.; McGrath, J. E. *Chem Rev* 2004, 104, 4587.
4. Kim, Y. S.; Sumner, M. J.; Harrison, W. L.; Riffle, J. S.; McGrath, J. E.; Pivovar, B. S. *J Electrochem Soc A* 2004, 151, 2150.
5. Einsla, B. R.; Kim, Y. S.; Hickner, M. A.; Hong, Y. T.; Hill, M. L.; Pivovar, B. S.; McGrath, J. E. *J Membr Sci* 2005, 255, 141.
6. Fu, Y.; Manthiram, A.; Guiver, M. D. *Electrochem Commun* 2006, 8, 1386.
7. Asano, N.; Aoki, M.; Suzuki, S.; Miyatake, K.; Uchida, H.; Watanabe, M. *J Am Chem Soc* 2006, 128, 1762.
8. Zhang, W.; Gogel, V.; Friedrich, K. A.; Kerres, J. *J Power Sources* 2006, 155, 3.
9. Kim, Y. S.; Einsla, B.; Sankir, M.; Harrison, W.; Pivovar, B. S. *Polymer* 2006, 47, 4026.
10. Park, H. B.; Lee, C. H.; Sohn, J. Y.; Lee, Y. M.; Freeman, B. D.; Kim, H. J. *J Membr Sci* 2006, 285, 432.
11. Fu, Y. Z.; Manthiram, A. *J Power Sources* 2006, 157, 222.
12. Krishnan, N. N.; Kim, H. J.; Prasanna, M.; Cho, E.; Shin, E. M.; Lee, S. Y.; Oh, I. H.; Hong, S. A.; Lim, T. H. *J Power Sources* 2006, 158, 1246.
13. Kim, H. J.; Krishnan, N. N.; Lee, S. Y.; Hwang, Y.; Kim, D.; Jeong, K. J.; Lee, J. K.; Cho, E.; Lee, J.; Han, J.; Ha, H. Y.; Lim, T. H. *J Power Sources* 2006, 160, 353.
14. Kim, D. S.; Kim, Y. S.; Guiver, M. D.; Pivovar, B. S. *J Membr Sci* 2008, 321, 199.
15. Easton, E. B.; Astill, T. D.; Holdcroft, S. *J Electrochem Soc A* 2005, 152, 752.
16. Jung, H. Y.; Cho, K. Y.; Sung, K. A.; Kim, W. K.; Park, J. K. *J Power Sources* 2006, 163, 56.
17. Jung, H. Y.; Cho, K. Y.; Sung, K. A.; Kim, W. K.; Kurkuri, M.; Park, J. K. *Electrochim Acta* 2007, 52, 4916.
18. Seland, F.; Berning, T.; Børresen, B.; Tunold, R. *J Power Sources* 2006, 160, 27.
19. Sasikumar, G.; Ihm, J. W.; Ryu, H. *J Power Sources* 2004, 132, 11.
20. Sumner, J. J.; Creager, S. E.; Ma, J. J.; DesMarteau, D. D. *J Electrochem Soc* 1998, 145, 107.
21. Sumner, M. J.; Harrison, W. L.; Weyers, R. M.; Kim, Y. S.; McGrath, J. E.; Riffle, J. S.; Brink, A.; Brink, M. H. *J Membr Sci* 2004, 239, 199.
22. Ueda, M.; Toyota, H.; Ouchi, T.; Sugiyama, J.; Yonetake, K.; Masuko, T.; Teramoto, T. *J Polym Sci Part A: Polym Chem* 1993, 31, 853.
23. Wen, H. L.; Song, C. S.; Tong, Y. F.; Chen, L.; Liu, X. L. *J Appl Polym Sci* 2005, 96, 489.
24. Gil, M.; Ji, X.; Li, X.; Na, H.; Hampsey, J. E.; Lu, Y. *J Membr Sci* 2004, 234, 75.
25. Harrison, W. L.; Wang, F.; Mecham, J. B.; Bhanu, V. A.; Hill, M.; Kim, Y. S.; McGrath, J. E. *J Polym Sci Part A: Polym Chem* 2003, 41, 2264.
26. Shao, Y.; Yin, G.; Wang, Z.; Gao, Y. *J Power Sources* 2007, 167, 235.
27. Ma, C. S.; Zhang, L.; Mukerjee, S.; Ofer, D.; Nari, B. D. *J Membr Sci* 2003, 219, 123.
28. Zhang, L.; Ma, C.; Mukerjee, S. *Electrochim Acta* 2003, 48, 1845.
29. Ciureanu, M.; Roberge, R. *J Phys Chem B* 2001, 105, 3531.
30. Song, J. M.; Cha, S. Y.; Lee, W. M. *J Power Sources* 2001, 94, 78.